Plasma Dynamics

19. Plasma Dynamics

Academic and Research Staff

Prof. T.M. Antonsen, Jr., Prof. G. Bekefi, Prof. A. Bers, Prof. B. Coppi, Prof. T.H. Dupree, Prof. L.M. Lidsky, Prof. J.E. McCune, Prof. M. Porkolab, Prof. L.D. Smullin, Dr. S. Atzeni, Dr. R.H. Berman, Dr. G. Bertin, Dr. G.A. Bonizzoni, Dr. P.T. Bonoli, Dr. T. Boutros-Ghali, Dr. C.M. Celata, Dr. K-I, Chen, Dr. V. Colomer, Dr. R.C. Englade, Dr. M. Gerver, Dr. K. Hizanides, Dr. J.H. Irby, Dr. R.E. Klinkowstein, Dr. V.B. Krapchev, Dr. J.S. Levine, Dr. S.C. Luckhardt, Dr. A. Palesky, Dr. F. Pegoraro, Dr. P.A. Politzer, Dr. A.K. Ram, Dr. J. Ramos, Dr. M.E. Read, Dr. B. Richards, Dr. G. Rubinacci, Dr. N.N. Sharky, Dr. R.E. Shefer, Dr. V. Stefan[7], Dr. L.E. Sugiyama, Dr. D.J. Tetreault, E.W. Fitzgerald, I. Mastovsky, Y.Z. Yin, M.-L. Xue

Graduate Students

J.G. Aspinall, A.A. Awwad, M. Baghaii Anaraki, P.E. Cavoulacos, B. Chike-Obi, D.E. Coate, K.D. Cogswell, G.B. Crew, A.K. Ezzedine, J. Fajans, A. Ferreira, A.S. Fisher, M.E. Foord, G. Francis, R.C. Garner, T.R. Gentile, P.J. Gierszewski, K.E. Hackett, L.P. Harten, D. Hinshelwood, R.S.-C. Hu, D.K. Ingram, N.A. Ismail, K.D. Jacobs, J.L. Jones, D.A. Kirkpatrick, S.E. Kissel, S.F. Knowlton, G.D. Krc, B.L. LaBombard, B. Lane, A.S. Leveckis, W.P. Marable, M.E. Mauel, M.J. Mayberry, F.S. McDermott, A. Pachtman, S.J. Piet, R.E. Potok, C.M. Rappaport, P.B. Roemer, R.R. Rohatgi, S.E. Rowley, S.R. Shanfield, M.D. Stiefel, G.M. Svolos, D.R. Thayer, C.E. Thomas, T. Uchikawa, S.H. Voldman

19.1 Relativistic Electron Beams and Generation of Coherent Electromagnetic Radiation

National Science Foundation (Grant ECS82-00646)
U.S. Air Force - Office of Scientific Research (Contracts AFOSR-82-0053 and F49620-83-C-0008)
Sandia National Laboratory (Contract 31-5606)
George Bekefi, Ruth E. Shefer

This group is concerned with the generation of intense, coherent electromagnetic radiation in the centimeter and millimeter wavelegth range. The primary radiation mechanism which is being studied at the present time is the free electron laser instability which is excited when an electron beam passes through a spatially periodic, transverse magnetic field (wiggler field). This instability is characterized

[7] Visiting Scientist from Boris Kidric Institute, Belgrade, Yugoslavia

by axial electron bunching and has emission wavelengths associated with the Doppler upshifted wiggler periodicity.

The experimental facilities include three pulsed high voltage accelerators capable of delivering up to 100 kA of current at 0.5 to 1.5 MV. Their characteristics are summarized below:

Pulserad 110 A

Voltage	1.5 MV
Current	20 kA
Pulse Length	30 ns

Pulserad 615 MR

Voltage	0.5 MV
Current	4 kA
Pulse Length	1μs

Nereus

Voltage	0.6 MV
Current	100 kA
Pulse Length	30 ns

Intense coherent sources of centimeter and millimeter wavelength radiation find applications in many diverse fields of research and technology including heating and diagnostics of thermonuclear fusion plasmas, photochemistry, solid state physics, and biophysics. One advantage of free electron systems such as the free electron laser are the very high predicted efficiencies which may be attained. Another important advantage is frequency tunability which results from the fact that the radiation frequency is not locked to an atomic or molecular transition or to an electromagnetic mode of a resonant structure but is instead determined by the velocity of the beam electrons.

The research being carried out by this group focuses on some of the basic issues in the development of free electron sources: the interaction of electron beams with different wiggler field geometries, resonant efficiency enhancement in the presence of a uniform guiding magnetic field, effects of beam emittance and velocity spread on the interaction, and the development of cross-field free electron lasers. In addition, the physics of high current field emission diodes which are commonly used as electron sources for intense beams is being studied. Recent work in these areas is summarized in the following sections.

a. The Rippled Field Magnetron (Cross-Field Free Electron Laser)

To achieve efficient conversion of energy from a stream of free electrons to electromagnetic radiation, near synchronism must be attained between the velocity of the electrons and the phase velocity of the wave. In cross-field devices, of which the magnetron is a typical example, this synchronism occurs between electrons undergoing a $v = E_0 \times B_0$ drift in orthogonal electric and

magnetic fields, and an electromagnetic wave whose velocity is reduced by a slow-wave structure comprised of a periodic assembly of resonant cavities. The complex system of closely spaced resonators embedded in the anode block limits the conventional magnetron to wavelengths in the centimeter range. Moreover, at high voltages typical of relativistic magnetrons, RF or dc breakdown in the electron beam interaction space, and at the sharp resonator edges poses serious problems.

The rippled-field magnetron is a novel source of coherent radiation devoid of physical slow-wave structures and capable of radiating at much higher frequencies than a conventional magnetron. The configuration of the anode and cathode is similar to the so-called "smooth-bore" magnetron, but it differs from the latter in that the electrons are subjected to an additional field, an azimuthally periodic (wiggler) magnetic field B_ω oriented transversely to the flow velocity v. The resulting $-ev \times B_\omega$ force gives the electrons an undulatory motion which effectively increases their velocity, and allows them to become synchronous with one of the fast TE or TM electromagnetic modes (phase velocity > c) characteristic of the smooth-bore magnetron.

We note that this interaction is the basis of free-electron lasers (FEL). This device differs from the conventional FEL in that the electron source (the cathode) and the acceleration region (the anode-cathode gap) are integral parts of the RF interaction space. This makes for high space-charge densities and for large growth rates of the FEL instability.

The magnetron configuration is cylindrical rather than linear as in conventional FEL's, and the system is therefore very compact. The cylindrical geometry also allows for a continuous circulation of the growing electromagnetic wave, and because of this internal feedback, the rippled-field magnetron is basically an oscillator rather than an amplifier as is the case of the FEL.

We have obtained measurements of millimeter-wave emission from the rippled field magnetron. In these experiments the magnetic wiggler field is produced by a periodic assembly of samarium-cobalt bar magnets positioned behind the smooth, stainless steel electrodes. Maximum radiated power in the 26.5-60 GHz frequency band is obtained with a wiggler periodicity of 2.53 cm and a wiggler field amplitude of 1.96 kG. Under these conditions a narrow band spectral line is observed with a line width at the half power points of less than 2.2 GHz. The center frequency of this line can be varied from 32 GHz to 46 GHz by varying B_z between 5.8 kG and 9 kG. No deterioration in line profile is observed over this range. The total radiated power above 26.5 GHz measured with this wiggler is 300 kW; which is more than a factor of thirty above the broad-band noise observed with no wiggler.

b. Low Voltage Free Electron Laser

Many theoretical studies have been devoted to free electron lasers comprised of an electron stream traversing a periodic, circularly polarized magnetic (wiggler) field, as can be generated with bifilar, helical, current-carrying wires. The electron dynamics in these systems exhibit simple properties that have considerable theoretical appeal. However, from the experimental point of view large amplitude,

circularly polarized wiggler fields are difficult to attain because of the large currents that are required in their windings; and for long pulse or steady-state operation, bifilar conductors may be entirely out of the question. In view of the above, studies of free electron lasers have begun in which the electron beam is subjected to a periodic, linearly polarized transverse magnetic field such as can be produced, for example, by an assembly of permanent magnets. Indeed, the use of samarium-cobalt as the magnet material has led to a new generation of magnetic wiggler systems.

Our experimental and theoretical studies are concerned with a low voltage free electron laser in which the electron beam is guided by an axial magnetic field and is perturbed by a linearly polarized samarium-cobalt wiggler field. Typical parameters which we hope to attain are given in Table 1 below:

Table 1. Summary of FEL parameters

Beam voltage (kV)	30
Beam current density (Acm^{-2})	22.3
Axial magnetic field (kG)	1.0
Wiggler field (kG)	0.20
Period of wiggler (cm)	2.0
Radiation wavelength (cm)	5.17
Spatial growth rate of TE mode (dB/M)	20.0
Spatial growth rate of TEM mode(dB/M)	12.2
Efficiency TE mode (%)	63
Efficiency TEM mode (%)	63

This experiment is now in the final stages of assembly. The electron beam is produced by a commercially available electron gun, with slight modifications. The beam has a diameter of 2 mm, and a current of 0.7A when operated at its rated 30 kV. Although the gun is capable of being run continuously, it is currently operated in pulsed mode. The pulse width is variable from 1-5 μsec, with a 0.001 duty cycle.

An axial magnetic field, generated by a series of 15 water-cooled electromagnetic coils guides the electron beam down a 1.5 m long conducting pipe. This uniform field can be varied from 0 to greater than 3 kG.

The linear wiggler magnetic field is produced by 480 $SmCo_5$ permanent magnets. The wiggler has been designed with a great deal of flexibility. It's overall length is 1.2 m, with the 10 cm at each end having an adjustable gap in order to taper the strength of the wiggler as desired. The design

periodicity is 2.0 cm, but the permanent magnets can be rearranged to give shorter and longer periodicities. With a 2.0 cm period, the wiggler field amplitude can be varied from 50 G to 1 kG.

A great deal of attention has been given to the uniformity of the wiggler. Detailed measurements of the individual $SmCo_5$ magnets, and of the assembled wiggler, have led to a thorough understanding of the wiggler. Upon completion, the wiggler field amplitude should be uniform to within 1% at the peaks of all the periods.

When the free electron laser is fully operational, microwave radiation at a frequency of approximately 6 GHz will be measured using crystal detectors. Power and frequency measurements will be made with heterodyning techniques.

The motion of the electrons themselves will be monitored with a Faraday cup. At these low beam voltages, it is possible to use a repelling grid in the cup. This will allow for measurement of the axial velocities of the electrons, and thus a determination of the electron distribution function.

Measurements of the microwave radiation and the electron ballistics will be made simultaneously, enabling correlations between the two to be accurately investigated. All measurements will be carried out for a variety of experimental parameters, including wiggler strength, radiation polarization, and proximity to resonance. When this resonance condition is satisfied, the cyclotron wavelength of an electron in the uniform guiding magnetic field equals the wiggler periodicity. Enhanced growth of the radiation field is predicted as this condition is approached.

c. Velocity Diagnostics of Mildly Relativistic, High Current Electron Beams

The past ten years have seen a great deal of interest in the production of high power millimeter and submillimeter wavelength radiation with free electron devices such as the gyrotron and the free electron laser. In contrast with conventional microwave tubes which typically use 1–10 keV, milliampere beams, these devices employ 50 keV–2 MeV electron beams with current densities of up to tens of kiloamperes per square centimeter. In addition, their operating efficiency is extremely sensitive to the electron velocity components in the beam. We have investigated two velocity diagnostic techniques which may be used with high energy, high current density beams. Both diagnostics have been successfully tested on an electron beam with an energy of 400–1200 keV carrying a current of 1–2 kA.

The first technique involves a simultaneous measurement of the beam current and radial electrostatic potential. The beam current is measured with a Rogowski coil or a current viewing resistor, and the potential is determined from the voltage across a cylindrical capacitor coaxial with the beam. These measurements allow one to determine the time resolved, spatially averaged axial streaming velocity $v_{\parallel}$ in the beam.

The second diagnostic measures the electron cyclotron wavelength in a beam propagating in a uniform guiding magnetic field. This is accomplished by placing a small pinhole aperture in the path of the beam, and a moveable collector of comparable diameter downstream of the pinhole. The observed spatial periodicity of the collected current allows one to calculate the product $\gamma v_{\parallel}$ in the beam. Here $\gamma = [1 - v_{\parallel}^2/c^2 - v_{\perp}^2/c^2]^{-1/2}$ and $v_{\perp}$ is the transverse velocity component.

We note that the capacitive velocity probe yields information about $v_{\parallel}$ alone, whereas the cyclotron wavelength probe measures a combination of $v_{\parallel}$ and $v_{\perp}$. By combining the two diagnostics, a full description of the electron beam may be obtained. This has been the major aim of our experiments.

d. Cathode Plasma Properties

The properties of the plasma layer formed on the cathodes of pulsed vacuum diodes determine many aspects of the behavior of these devices. Electron flow may be affected by plasma nonuniformity or by plasma instabilities, and the diode pulse length is often limited by gap closure due to expansion of the cathode plasma. The electron flow and gap closure in turn affect the performance of intense ion beam diodes, magnetically insulated transmission lines and intense electron beam driven microwave devices. To control these effects it becomes necessary to control the uniformity, composition, density and temperature of the cathode plasma.

A relevant question concerns the importance of surface contaminants such as the thin layers of pump oils which will exist in most practical vacuum systems. If these impurities dominate cathode plasma formation then variations in cathode material and surface preparation will have little effect on the cathode plasma properties.

We are studying the influence of diode current density, cathode material, cathode surface preparation and diode vacuum condition on the properties of the cathode plasma in a pulsed electron beam diode energized by a Nereus accelerator. The cathode plasma density has been observed to be dependent on the cathode material and to increase with increasing current density. Plasma formation has been observed to occur during the entire diode power pulse. Both electrode materials and constituents of surface contaminants are observed in the cathode plasma. Fast ions have also been observed, moving within the cathode plasma from the cathode toward the anode with kinetic energies far exceeding that which would be expected from a thermal expansion of the cathode plasma.

19.2 Nonlinear Wave Interactions—RF Heating and Current Generation in Plasmas

National Science Foundation (Grants ENG79-07047 and ECS82-00646)
U.S. Department of Energy (Contract DE-AC02-78ET-51013)
Abraham Bers, Vladimir Fuchs[8], Dennis Hewett[9], Kyriakos Hizanidis, Vladimir Krapchev, Abhay Ram, V. Stefan[10], Gregory Francis, Leo Harten

The past year has witnessed a major breakthrough in experiments on current drive in tokamak plasmas with externally excited lower-hybrid waves. The two outstanding results were from the Princeton PLT group (400 kWatt of rf power generating 165 kA of plasma current for 3.5 sec, and 420 kAmp for 0.3 sec; plasma density $10^{13}/cm^3$, plasma major radius 1.32 m) and from the M.I.T. Alcator C group (1 MWatt giving 200 kAmp for 0.2 sec in a plasma of density $10^{14}/cm^3$ and major radius 0.64 m. In both experiments the currents are carried by very energetic electrons (100-500 keV)—a hundred times, or more, the bulk plasma temperature. In addition, both experiments show that the current carrying electrons have a large spread in their energies perpendicular to the magnetic field, i.e., effective perpendicular temperatures that are 50-100 times the bulk plasma temperature. Both of these features were not foreseen, and cannot be adequately described, by presently available theoretical models. We have initiated theoretical work and computations aimed at a proper two-dimensional (velocity-space) description of RF current drive including relativistic dynamics of the current-carrying electrons. Our results to date are given in subsections (a) and (b).

A basic problem in either energy deposition (i.e., heating) or momentum deposition (i.e., current drive) by RF in a plasma concerns the calculation of an effective particle diffusion coefficient induced by the RF fields. In the past year we have initiated a numerical study of a simple model for electrons interacting with a wavepacket. The results indicate that with increasing RF field amplitude a transition occurs from a quasilinear to a new nonlinear regime in which the diffusion is much reduced and perhaps not even well-defined. The results are described in subsection (c).

During the past year we have also formulated a relativistic generalization of the criteria that distinguish absolute from convective evolutions of instabilities. This opens up a way of studying electromagnetic instabilities in relativistic plasmas, and is summarized in subsection (d).

Finally, in subsection (e) we report on the completion of our analytical and computational work related to RF coupling for ion-cyclotron heating of plasmas.

---

[8]Visiting Scientist from IREQ - Hydroquebec, Monreal, Canada

[9]Plasma Fusion Center, M.I.T.

[10]Visiting Scientist, Boris Kidric Institute, Belgrade, Yugoslavia

a. Steady State Solution of the Two-Dimensional Fokker-Planck Equation with RF Diffusion

We have studied analytically and numerically the 2D Fokker-Planck equation with an RF diffusion. The results are directly applicable to the problem of lower-hybrid current drive in a tokamak. Previously reported[1] numerical results fail to exhibit important differences between the one-dimensional and two-dimensional theories. Our 2D study shows that there is a significant broadening of the distribution function in the perpendicular direction. The perpendicular temperature ($T_\perp$) in the resonant domain is much greater, often by an order of magnitude, compared with the bulk electron temperature T_B}.[2,3] As a result both current (J) and power dissipated (P) are enhanced in 2D theory, compared to the 1D result by the factor:

$$J_{2D} \approx J_{1D}\, T_\perp / T_B\,,\quad P_{2D} \approx P_{1D}\, T_\perp / T_B \tag{19.1}$$

where $J_{2D}(J_{1D})$ is the current in 2D(1D) theory and $P_{2D}(P_{1D})$ is the power dissipated in 2D(1D) theory. We note that the figure of merit J/P is unchanged from the one previously reported.[1] The importance of our results lies in the fact that it allows us to explain the observed current with significantly smaller change in the position of the power spectrum launched by the waveguide array.

b. The Relativistic Generalization of the Two-Dimensional Fokker-Planck Equation with RF Diffusion

The relativistic generalization of the quasilinear theory of current drive[1] is motivated by the fact that the RF spectra in Alcator C, PLT (and certainly in future reactor scale devices) have phase velocities that extend into regions where relativistic effects must be taken into account. In Alcator C and PLT the accessibility wave number of the excited spectrum implies a phase velocity resonant with particles of 170 and 500 keV respectively, while the corresponding lowest resonant energies (highest wave numbers) are about 30 keV. However, inside the plasma it is necessary that the spectrum extend below 30 keV and eventually connect to the thermal bulk (of 1 keV) at energies near 5 keV. Several mechanisms have been proposed to account for the existence of rf fields at phase velocities in this gap between 30 keV and 5 keV. We have been mainly concerned with a proper treatment of the more energetic electrons that carry the major part of the current.

The current generated by the applied rf field is mainly carried by energetic electrons in the tail of the distribution function since these are the particles which resonate with the applied field while the thermal bulk remains more or less unaffected (Maxwellian). The energetic particles experience collisions with the thermal electrons and ions as well as quasilinear diffusion (QD) due to the RF spectrum. The relativistic Fokker-Planck (FP) operator which describes the thermalization of highly energetic electrons generated by the RF is formulated on the basis of the relativistic Balescu-Lenard collision operator[4] taken in the Landau limit. The Landau operator, which acts in momentum-space, has further been expanded keeping terms of order up to $(p_{\text{thermal}}/p_{\text{tail electrons}})^2$. We thus obtain a Fokker-Planck operator which in the limit of a cold background plasma is reduced to that of Mosher.[5]

The energy, momentum and velocity moments of the relativistic Fokker–Planck operator provide the relaxation rates of the average energy, average momentum and current respectively, carried by the energetic tail electron. In a steady state operation one requires all these three relaxation mechanisms to balance the RF power and momentum being fed to the electron. For the nonrelativistic limit, the momentum and velocity relaxation are identical. By solving the related three balance equations one obtains the RF power and the current generated as function of the average kinetic energy of the tail electrons as well as the figure of merit, namely, the ratio of the current generated to the power dissipated. We thus find:

$$\left(\frac{I}{P_D}\right)_{Amp/Watt} = \frac{3I.2}{\ln\Lambda_t} \frac{f(\varepsilon)}{R_m n_{20}} \tag{19.2}$$

where $\ln\Lambda_t$ is the Coulomb logarithm for the tail electrons, R_m is the major radius of the plasma in meters, n_{20} is the plasma density in units of $10^{20}/m^3$; the function $f(\varepsilon)$, of the particles' energy, is

$$f(\varepsilon) \equiv \frac{(\varepsilon+1)^2 - 1}{(\varepsilon+1)^{3/2}(\varepsilon+2+Z_i)^{1/2}} \tag{19.3}$$

where $\varepsilon = (\mathcal{E}_0/mc^2)$ is the effective energy $\mathcal{E}_0$ of the current carrying electrons normalized to the rest energy, and Z_i is charge number of the ions in the bulk plasma.

We have also solved the combined Fokker–Planck and quasilinear diffusion equation modeling the distribution function by $f_{\|}(p_{\|},p_{\perp}) = \exp[-p_{\perp}^2/2m_e T_{\perp}(p_{\|})] F(p_{\|})/2\pi m_e T_{\perp}(p_{\|})$ where $p_{\|}$, $p_{\perp}$ and $T_{\perp}(p_{\|})$ are the parallel, perpendicular to the magnetic field momenta and perpendicular temperature, respectively. In this ansatz we then allow a $p_{\|}$–dependence of $T_{\perp}$. In fact, this is borne out by recent experiments on PLT which indicate perpendicular temperatures of the current carrying tail electrons considerably higher than the temperature at the thermal bulk.[6] Integrating the Fokker–Planck equation over $p_{\perp}$ we obtain an equation for $F(p_{\|})$ which generalizes the one–dimensional nonrelativistic results. Combining the general solution for $F(p_{\|})$ with the perpendicular energy moment of the FP + QL equation we obtain an equation for $T_{\perp}(p_{\|})$ which is then solved numerically. Our model predicts a considerable perpendicular temperature in the region where the RF spectrum applies, the maximum of which depends very sensitively on the width of the spectrum. For example, for an average diffusion coefficient $D_0 = 10$ (normalized to the bulk collisional diffusion) referred to a spectrum centered at $p_0 = 10$ and having a width $\Delta p = 10$ (both normalized to the thermal momentum) we predict a temperature profile with a maximum $T_{\perp}$ about 7.5 T_{BULK}, while for $p_0 = 15$, $D_0 = 5$ and $\Delta p = 20$ the maximum $T_{\perp}$ is about 28 T_{BULK}.

c. Diffusion and Current Generation by Coherent Wavepackets

The momentum transfer and diffusion of electrons periodically interacting with a coherent longitudinal wavepacket is considered.[8,9] Applying the resonance overlap criterion, we establish the

stochastic threshold and the stochastic region Δ_{stoch} in velocity space.[10] Discrete mapping and direct numerical integration of the single-particle dynamics is used to corroborate the resonance overlap results and to find the momentum transfer to, and diffusion of, electrons in the field. Above a certain threshold, which depends on field strength, spectrum width and electron cycling length, the interaction is non-adiabatic and particle motion is stochastic within a bounded, not necessarily simply-connected, region of velocity-space. The nature of the interaction, and also the source of stochasticity, depends on the ratio of two basic time scales in the problem: the particle transit time through the wavepacket which is also the autocorrelation time τ_{ac}, and the particle bounce time τ_b in the wavepacket.

When $\tau_{ac} \ll \tau_b$, the particle-velocity scattering is everywhere local in velocity-space and the diffusion approximation holds. An increase in $\langle v \rangle$ and $\langle \delta v^2 \rangle$ is positively correlated with the onset of stochasticity. We find a net induced current $j \sim \Delta v_{stoch}$ and in the weak-field regime an initial rate of change of the variance $\langle \delta v^2 \rangle / 2t$ equal to the quasilinear-theory diffusion coefficient.[11] In the strong-field regime momentum transfer and stochasticity persist owing to nonadiabatic transitions between trapped and untrapped states as the electron traverses the wavepacket. The diffusion coefficient substantially deviates from the quasilinear value, scaling approximately as the square root of the field strength. In general, however, the scattering in v-space tends to lose its local, diffusive character.

d. Pulse Shapes of Absolute and Convective Instabilities for Relativistic Observers

The problem of describing the propagation of an instability in a plasma and, in particular, of deciding between convective and absolute instabilities has been of considerable interest.[12] The qualitative aspects of determining linear instabilities and distinguishing between the absolute and convective instabilities by using the pinch-point analysis has already been developed.[13] The space-time asymptotic pulse shape for these instabilities has been obtained for non-relativistic observer velocities.[14] Such an analysis is strictly applicable to electrostatic instabilities involving non-relativistic dynamics of the plasma particles. We have developed the generalization to the relativistic theory for the asymptotic pulse evolution which is applicable to electromagnetic instabilities in plasmas involving relativistic dynamics.[15,16] The theory has been applied to the studies of instabilities in an infinite plasma immersed in a static uniform magnetic field ($\vec{B_0}$) with stationary ions and highly anisotropic electron distribution functions. We have looked at instabilities that propagate parallel to $\vec{B_0}$ and perpendicular to $\vec{B_0}$ and evaluated their corresponding pulse shapes. The dispersion relation for these waves is derived from the complete set of Maxwell's equations and the relativistic Vlasov equation. The electromagnetic instabilities of the type considered are of interest in the studies of: the generation of electromagnetic energy by relativistic electron beams; instabilities due to ECRH heated energetic electrons in the end-plugs of tandem mirror plasmas; and unstable radiations in space plasmas.

e. Antenna-Plasma Coupling Theory for ICRF Heating

We have completed our analysis to determine the coupling characteristics of an external antenna structure (consisting of a current-carrying sheet protected from the plasma by an idealized Faraday Shield) to a plasma for the purposes of exciting the fast component of waves in the ion-cyclotron range of frequencies.[17,18] The analysis is carried out in the slab geometry with a current sheet of finite extent in the poloidal (y) and toroidal (z) directions while the shield and the plasma are assumed to be infinite in y and z. The plasma is described by its cold dielectric tensor with density ($n(x)$) and magnetic field ($B_0(x)$) inhomogeneities in the radial (x) direction. The major conclusions of our three-dimensional analysis are the following:

(A) The radiation impedance of the antenna

- is significantly modified by including the finite poloidal extent of the antenna
- decreases with increasing $\nabla n(x)$ at the shield
- is an increasing function of the external rf source frequency (for a fixed $n(x)$ and electrical length of the current sheet)

(B) The plasma impedance is highly asymmetric with respect to the poloidal wave number. This implies that an appropriately phased set of poloidal antennas would allow more power to be coupled to the plasma.

(C) The excited electric and magnetic fields inside the plasma do not disperse significantly beyond the antenna dimensions.

References

1. C.F.F. Karney and N.J. Fisch, Phys. Fluids 22, 1817 (1979).
2. V. Krapchev, K. Hizanidis, A. Bers, and M. Shoucri, "Current Drive by LH Waves in the Presence of a DC Electric Field," Bull. Am. Phys. Soc. 27, 1006, (1982).
3. D. H. Hewett, V. Krapchev, J. P. Friedberg, and A. Bers, "Fokker-Planck Investigations of RF Current Drive," paper 1P10 Proc. 1983 Sherwood Theory Meeting, Arlington, Virginia.
4. K. Hizanidis, K. Molvig, and K. Swartz, M.I.T. Plasma Fusion Center Report PFC/JA-81-21 (1981) accepted for publication in J. Plasma Phys.
5. D. Mosher, Phys. Fluids 18, 846 (1975).
6. S. von Goeler, et al., Bull. Am. Phys. Soc. 27, 1069 (1982).
7. K. Hizanidis, V. B. Krapchev, and A. Bers, "Current Drive by Lower-Hybrid Waves Acting on Runaway Electron Tail," Bull. Am. Phys. Soc. 27, 1006, (1982).
8. K. Matsuda, in Proceedings of the Fourth Topical Conference of Radio-Frequency Heating in Plasmas, Austin, Texas, 1981, paper B10; also "Stochastic Current Drive by Plasma Waves, General Atomic Co. Report GA-A16303, July 1981.
9. T. H. Stix, in F. Sindoni (Ed.) Proceedings of the Third Symposium on Plasma Heating in Toroidal Devices, by (Editrice Compositori, Bologna, 1976), p. 159.
10. B. V. Chirikov, Phys. Reports 52, 263 (1979).
11. V. Fuchs, G. Thibaudeau, V. Krapchev, A. Ram, and A. Bers, "Diffusion and Momentum Transfer for Particles Interacting with Coherent Wavepackets," Bull. Am. Phys. Soc. 27, 957 (1982).

12. A. Bers, "Space-Time Evolution of Plasma Instabilities— Absolute and Convective," in Handbook of Plasma Physics, Vol. 1, Chapter 32, (North Holland Publishing Company) to be published 1983.
13. R. J. Briggs, Electron Stream Interaction with Plasmas, (M.I.T. Press, 1964).
14. L. S. Hall and W. Heckrotte, Phys. Rev. 166, 120 (1968).
15. A. Bers and A. K. Ram, "Relativistic Pulse Shapes of Absolute and Convective Instabilities," Bull. Am. Phys. Soc. 27, 919 (1982).
16. A. Ram and A. Bers, "Relativistic Evolution of Electromagnetic Instabilities," paper 2Q24, 1983 Sherwood Theory Meeting, Arlington, Virginia.
17. A. Ram and A. Bers, "Antenna-Plasma Coupling Theory for ICRF Heating of Large Tokamaks," Proceedings of Third Joint Varenna-Grenoble International Symposium on Heating in Toroidal Plasmas, Grenoble, France, March 22-27, 1982.
18. A. Ram, A. Bers, M.I.T. Plasma Fusion Center Report PFC/CP-82-2 (1982).

19.3 Tokamak Research: RF Heating and Current Drive

U.S. Department of Energy (Contract DE-AC02-78ET-51013)
George Bekefi, Miklos Porkolab, Stanley C. Luckhardt

The Versator II program consists of a number of diverse experiments on the interaction of externally excited lower-hybrid waves with a tokamak plasma. The lower-hybrid wave has a frequency between the electron and ion cyclotron frequencies and is introduced into the plasma with an antenna consisting of a phased array of waveguides. By adjustment of the relative phase between adjacent waveguides, $\Delta\Phi$, the spectrum of waves in $k_{||}$, where $k_{||}$ is the wave number parallel to the magnetic field, can be controlled.

The lower-hybrid wave can interact with either plasma electrons or ions depending on the wave phase velocity and the particle velocity. Wave-electron interaction occurs for electrons with parallel velocity, $v_{||} \simeq \omega/k_{||}$, in resonance with the wave phase velocity. This interaction allows lower-hybrid wave power to be deposited into plasma electrons which can heat the plasma. The wave interaction also increases the parallel momentum of the electrons and reduces their collisionality; and these effects allow the wave to drive a net electron current. The lower-hybrid wave electron interaction is seen to have two applications to tokamak fusion research. The RF current drive effect may allow a tokamak fusion reactor to operate in steady state with the needed plasma current driven by waves instead of inductively driven by a transformer, and wave power deposited in the electrons can heat the plasma supplying some of the temperature increase needed to reach fusion conditions, $T \simeq 10$ KeV.

The lower-hybrid wave can also interact with the ion population if the plasma density and magnetic field are sufficiently high. The lower-hybrid wave obeys the dispersion

$$\omega^2 = \omega_{LH}^2\left(1 + \frac{Mi}{Me}\frac{k_{||}^2}{K^2}\right) \tag{19.4}$$

where ω_{LH} is the lower hybrid resonance frequency,

$$\omega_{LH}^2 = \frac{\omega_{pi}^2}{1 + \omega_{pe}^2/\omega_{ce}^2} \tag{19.5}$$

Ion interaction occurs for ions with velocity $V_i = \omega/k_\perp$, the wave can interact with ions having much lower velocity than electrons since the $k_\perp$ of the wave reaches very large values, $k_\perp \gg k_\parallel$, when $\omega \sim \omega_{LH}$. Thermal effects also modify the dispersion relation when $\omega \sim \omega_{LH}$ leading to possible conversion of the lower-hybrid wave into a "hot plasma" wave, this wave also interacts with the ion component. The lower-hybrid wave-ion interaction, in principle, could also be useful for heating a plasma toward fusion temperatures; though, so far, lower-hybrid ion heating has not been reliably demonstrated in experiments.

Versator II is a medium sized research tokamak with the following parameters: major radius R_o = 40.5 cm, limiter radius a = 13 cm, toroidal field = 15 kGauss, plasma current = 30-60 kA.

The lower-hybrid RF system used in the current experiments consists of a 150 kW, 800 MHz klystron, and a waveguide power splitter with four output channels. The phase of each output can be continuously adjusted (0°-360°) with mechanical phase shifters. Such phase control allows traveling wave spectra to be launched either parallel or anti-parallel to the direction of the electron ohmic drift, $\Delta\Phi = \pm 90°$, or a standing wave spectrum can be excited with $\Delta\Phi = 180°$.

The results of earlier experiments can be summarized as follows: in the Versator experiments a significant fraction of the ohmic heating current was replaced by RF generated current in a regime of low density. Above $\bar{n}_{crit} = 6 - 7 \times 10^{12} cm^{-3}$ a significant decrease in current drive efficiency was observed.[1] During LHCD (lower-hybrid current drive)in the low density regime, the Parail-Pogutse tail anisotropy instability[2] was observed and was found to cause periodic losses of a significant fraction of the tail current.[3] In combined LHCD and electron cyclotron heating experiments on Versator II, it was found that the tail mode could be stabilized by addition of electron cyclotron heating, $P_{ECH} \gtrsim 20$ kW, and the periodic current losses were eliminated.[3] In recent experiments, a novel antenna arrangement was used to launch waves from the top of the torus.

19.3.1 Top Launching Experiments

Ray tracing theory[4,5,6] has shown that traveling waves launched from the top of the torus in the direction:

$$\vec{s} = \vec{B}\ I_p/|B|\,|I_p| \tag{19.6}$$

experience an upshift in their $N_\parallel = ck_\parallel/\omega$ due to toroidal effects. Generally, as a wave launched in this way propagates toward the center of the plasma it slows down along field lines, and is often absorbed in the first poloidal transit through the center of the plasma. Waves launched from the top

in the $-\vec{s}$ direction suffer a large downshift of $N_{||}$. Similarly, waves launched from the outer midplane of the torus suffer an initial $N_{||}$ downshift, making first pass absorption less likely in present day tokamaks due to the difficulty in satisfying the Landau damping resonance condition. In typical cases, side launched waves make many poloidal passes before they are completely absorbed; in general, some RF power may be lost (e.g. due to collisional absorption at the plasma edge). Thus, top launching is expected to give an improved power absorption efficiency and an interaction with lower energy electrons, when compared with side launching.

The $N_{||}$ upshift, however, is expected to result in reduced current drive efficiency, as indicated by the simple quasi-linear theory result[7] (in practical units)

$$\frac{I_{RF}}{P_D} = \frac{17g}{N_{||f}^2 R_o n_{15}} \frac{kA}{kW} \tag{19.7}$$

where I_{RF} is the RF generated current, P_D is the power dissipated, $N_{||f}$ is the mean $N_{||}$ value of the absorbed power spectrum, R_o is the major radius in cm, n_{15} is the density in units $10^{15}cm^{-3}$, and g is a factor usually of order unity depending on the width of the absorbed wave spectrum. Thus, to maximize the RF generated current, absorption of lower $N_{||}$ components is desirable. It appears from the above considerations that the top launched traveling waves may be an efficient means of heating electrons; however, owing to their upshift in $N_{||}$ the current drive efficiency may be reduced when compared to the side launched waves. Measurement of this difference in current drive efficiency is then expected to be a first sensitive test of the prediction of the ray tracing theory.

The top launch coupler consists of a stainless steel four-waveguide array inserted into a top rectangular port of the Versator vacuum chamber. The waveguide gap size is 1 cm and the waveguide width is 21 cm. With 90° relative phasing between adjacent waveguides, a traveling wave spectrum with peak at $N_{||o} \simeq 8$ is launched. Due to space limitation in the port, a reduced width waveguide was used, leading to higher RF electric fields than in the previously used side coupler, which had a width of 24.5 cm. These higher RF electric fields initially caused a waveguide breakdown problem. A solid titanium waveguide array was installed, but the breakdown power level did not improve. Best results were obtained after a carbon coating was applied to the waveguide surfaces.[8] With this arrangement more than 100 kW of power, corresponding to a power density of 1.3 kW/cm^2, has been coupled into plasma without evidence of waveguide plasma formation or arcing. We find that the power handling capability of the antenna is seriously degraded by discharge cleaning of the tokamak vacuum chamber. However, when impurity control is provided by titanium deposition on the chamber walls and discharge cleaning is eliminated, this high power operation becomes possible.

In preliminary experiments with the top launch coupler, current drive measurements have been made in the low density regime, $\bar{n}_e < 10^{13}cm^{-3}$. Monitored signals show the usual characteristics of

RF generated currents. Loop voltage and plasma current measurements indicate voltage drops and plasma current increases during the RF pulse when traveling waves are launched in the electron drift direction. When waves are launched in the opposite direction little or no voltage drop is observed.

In Table I, a comparison of current drive obtained with the top launch and side launch couplers is presented. Both side and top launch grills are phased at 90° giving a peak in the launched $N_{||}$ spectrum at $N_{||o} = 8$. Comparison is made in terms of the scaling parameter S defined as

$$S = \frac{I_{RF}}{P_{NET}} \bar{n}_{15} R_o(cm) \tag{19.8}$$

in units of $kA/(kW \cdot cm^2) \times 10^{15}$ where I_{RF} is the RF generated current, P_{NET} is the net power coupled into the plasma, $\bar{n}_{15}$ is the average density in units of $10^{15} cm^{-3}$ and R_o is the major radius in cm. The theoretically predicted value for S then depends only on the characteristics of the absorbed power spectrum and absorption efficiency, from Eq. (19.4):

$$S = 17\, g\, \eta / N_{||f}^2 \tag{19.9}$$

where η is the power absorption efficiency, $P_{dissipated} = \eta P_{net}$, g is a dimensionless spectral shape factor usually of order unity, and $N_{||f}$ is the peak of the absorbed power spectrum taking all toroidal shifts into account. The observed values of S for the top launching experiment are significantly smaller than observed with the side coupler. In typical cases $S_{side}/S_{top} \sim 6 - 8$. This decrease in S appears to be consistent with a toroidal upshift in $N_{||}$.

Table 1

	Top Launch Grill	Side Launch Grill
$\Delta\varphi$	90°	90°
$N_{||o}$	8	8
$\bar{n}$	$6 \times 10^{12} cm^{-3}$	$4 \times 10^{12} cm^{-3}$
I_p	40 kA	32 kA
$\Delta V/V_L$	0.18	0.5
q(a)	5.8	7.2
$I_{RF} \simeq \Delta V/V\, I_p$	7.3 kA	16 kA
P_{NET}	45 kW	8 kW
$S = \bar{n}_{15} \frac{R_o I_{RF}}{P_N}$	0.039	0.32

Soft x-ray spectroscopic measurements of the intermediate energy range 1 keV < ε_γ < 25 keV indicate the formation of an electron tail during RF injection. In Fig. 19-1 the soft x-ray spectrum of an ohmic discharge shows a thermal feature, $\varepsilon_\gamma \lesssim 3$ kV, evidence of a small runaway component, $\varepsilon_\gamma > 5$ kV, and some metallic impurity line radiation. During RF injection an electron tail is formed as indicated by the factor of 5 – 10 enhancement in the x-ray spectrum in the energy range 5 – 15 keV. There is also a large enhancement in line radiation 4 keV < ε_γ < 8 keV, indicating a possible build-up of metallic impurities during the RF pulse; however, this increase does not significantly change the Z_{eff} of the discharge. Similar soft x-ray behavior is observed for both ± 90° phase RF injection. Tail formation in the energy range 3–15 keV is consistent with the expected upshift of the antenna $N_{||}$ spectrum, for $\Delta\Phi$ = +90°; however, the similarity of the soft x-ray spectra for ±90° does not appear to fit the simple ray tracing picture. Further experiments are needed to clarify this observation.

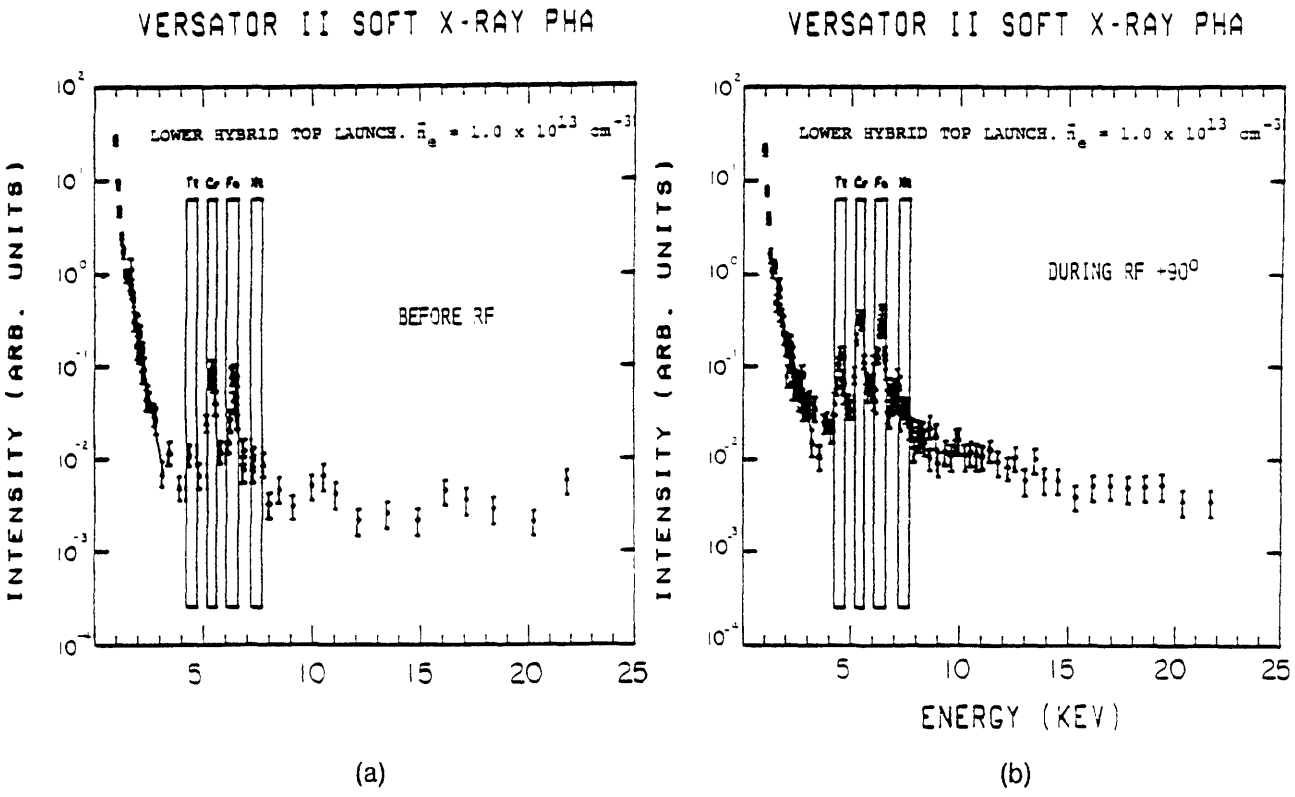

Figure 19-1: Soft x-ray spectra of
(a) ohmic discharge before RF pulse
(b) during injection of 45 kW of lower-hybrid power

19.3.2 Particle Confinement

Density increases have consistently been observed during lower-hybrid current drive (LHCD), e.g. Ref. 14. There are three apparent causes which could account for this density increase. They are: (1) increased recycling of hydrogen neutrals near the edge of the plasma (2) increased impurity influx and (3) improvement of particle confinement.

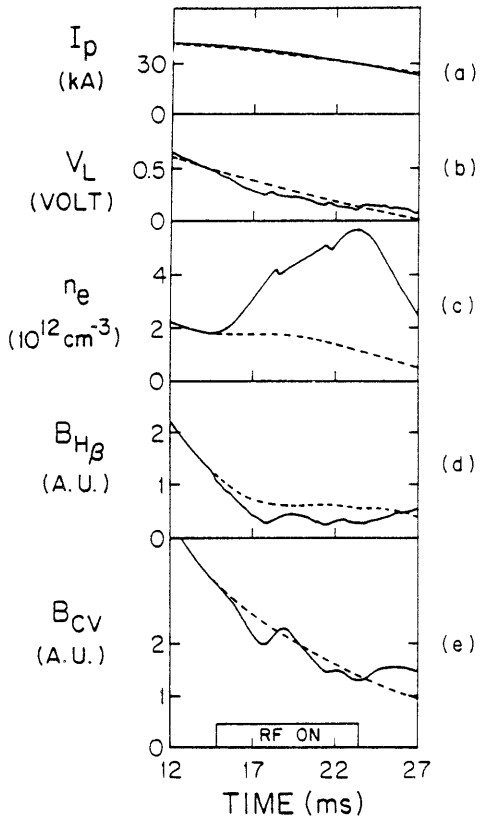

Figure 19-2: Temporal evolution of signals during the LHCD density increase:
(a) plasma current, (b) loop voltage, (c) density, (d) central chord brightness of H_β4661A, (e) central chord brightness of CV 2271A P_{RF} = 10 kω, $\Delta\varphi$ = +60°

The temporal evolution of plasma parameters and signals of relevant diagnostics are shown in Figs. 19–2 and 19–3. A 1/2 m Jarrel–Ash monochromator has been used to monitor neutral hydrogen emissions. Most measurements have been made with H_β(4861Å) line emission; however, both Hα(6563Å) and H_β have the same temporal dependences. During the RF pulse the density increases by ~ 100%in this case. Nevertheless, the H_β emission decreases by ~ 30 – 60% compared to ohmically heated discharges and then shows periodic small fluctuations. These variations on the H_β signal are correlated with loop voltage spikes and $2\omega_{ce}$ emission caused by the tail instability loss of electrons to the limiter and chamber walls. The decrease of H_β emission is consistent with the edge density decrease measured by a Langmuir probe (Fig. 19–3). The density increase during the RF has been simulated with gas puffing through a port located 158° toroidally away from the visible

monochromator port. The H_β emission increases in this case. Thus, if there is an extra neutral hydrogen flux introduced by the RF, the H_β emission should show a similar increase. The observed decrease of H_β emission and edge density during LHCD indicate the ionization rate at the plasma edge is decreasing even though the bulk density is increasing. Thus, the density build-up cannot be explained as an increase in gas flux or recycling.

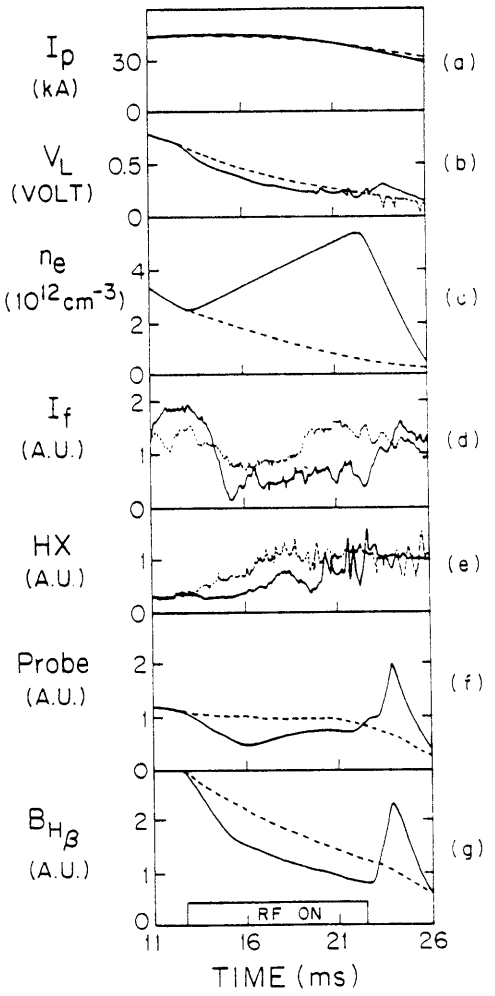

Figure 19-3: Temporal evolution of signals during LHCD density increase (a) plasma current, (b) loop voltage, (c) density, (d) density fluctuation level from 2 mm microwave scattering, fo = 325 kHz, (e) hard x-ray signal, (f) edge density from Langmuir probe, (g) central chord brightness of H_β

The behavior of light impurities has been monitored using the CV, OV, and CIII lines. CV emission has shown some slight decrease which might be related to a small decrease in electron temperature during the RF pulse, Ref. 1, or a reduced recycling rate for these impurities. Since impurity influx has to pass the plasma edge to reach the center, we would expect to observe an increase of all the edge lines if there is an increase in impurity flux. These measurements indicate that there is no increase in

light impurity influx during the RF. The remaining possible explanation of the observed density increase is an improvement in particle confinement. In the typical example shown in Fig. 19–3, the density increases by a factor of two and H_β emission decreases consistent with a factor of 2 – 4 increase in τ_p during LHCD. The "drift–wave" frequency range fluctuations are also observed to decrease during current drive. Fig. 19–3 shows fluctuation signals at 325 kHz averaged over a few shots with and without RF, respectively as obtained from 2 mm microwave scattering. The drop in fluctuation is conservatively estimated to be 5 dB.

In summary, the observed increase in plasma density cannot be fully explained as an increase in recycling or ionization; rather a decrease is observed. Neither is there any appreciable increase of light impurity influx. There is an accumulation of evidence consistent with a significant increase of particle confinement during LHCD.

19.3.3 Versator Upgrade

The successful production of an RF driven plasma current in Versator II gives rise to the possibility of tokamak operation sustained solely with RF power. At present a major construction project is underway on Versator II upgrading the magnetic field systems to allow a fully RF driven tokamak plasma to be produced.

The RF driven state will be reached by the following method: the tokamak discharge will be initiated with the ohmic heating transformer, producing an inductively driven plasma current; then after a 10–15 msec start–up phase, RF power will be injected into this target plasma to build up an RF driven component of the total current. During the build–up of the RF current, the current in the transformer primary will be brought to zero and the transformer will be open circuited. At this point maintenance of the plasma current is provided by RF current drive only. To insure that all inductively driven currents are eliminated, the total plasma current will be sustained with $dI/dt = 0$ for approximately two "L/R" times.

To make the transition from the inductively–driven discharge to the RF driven regime, the Versator II magnetic field systems and the RF power system will be upgraded to allow plasma equilibrium to be maintained for up to 60 msec; this will allow a 15 msec transition phase, and a 35 msec RF driven phase, limited only by the pulse duration of the toroidal field power supply.

19.3.4 S–Band Current Drive Experiment

Currently under construction for Versator II is a 2.45 GHz high frequency lower–hybrid current drive experiment. The purpose of this experiment is to determine whether the 800 MHz current drive density limit of $\bar{n}_e \lesssim 6 \times 10^{12} cm^{-3}$ first found on Versator II can be improved by raising the RF source frequency.

The 2.45 GHz RF system will consist of two 50 kW Varian 5K70SH–2 klystrons, along with a power

splitting and phase shifting network which will feed a 4-waveguide array. Present designs call for vacuum waveguide dimensions of .8 cm x 8.64 cm, which corresponds to a maximum injected power density of 3.6 kW/cm^2. The maximum pulse length will be 40 ms.

At the present time, fabrication of the high power RF system is under way, along with the design and procurement of the power monitoring and phase detection circuitry. Initial klystron testing and lower power coupling experiments are scheduled for the end of 1983, with high power current drive experiments commencing in 1984.

The new 2.45 GHz RF system will be capable of operating simultaneously with the present 800 MHz system to allow a detailed comparison of lower-hybrid current drive near the density limit at each frequency.

19.3.5 Tail Mode Instability

The Parail-Pogutse tail anisotropy instability is normally present during lower-hybrid current drive on Versator. In earlier experiments[3] it was shown that relaxation oscillations present on the loop voltage, second harmonic cyclotron emission, and other diagnostics were also accompanied by sudden losses of a significant fraction of the tail current during LHCD. It was also found that the addition of more than 20 kW of electron cyclotron heating power could stabilize the relaxation oscillations by increasing the tail $T_\perp$. These relaxation oscillations are also accompanied by intense RF bursts, measurable by an RF probe, occurring simultaneously with the sudden increases in $2\omega_{ce}$ emission and loop voltage. In present experiments the frequency spectrum of these RF bursts has been measured with an RF probe in the limiter shadow. The bursting is found to exist over a wide frequency range. In Fig. 19-4 the intensity of the RF bursts detected by the RF probe is plotted as a function of their frequency in a low density ohmic discharge, and during the LH power pulse with 10 kW of coupled power at $\Delta\Phi = 60°$. The frequency spectrum of the tail mode bursts appears to broaden from 9 GHz in the ohmic case to 12 GHz during LHCD. The spatial distribution of the high energy electron tail has been obtained with a scanning hard x-ray spectrometer. Massive lead collimators and vertical viewing into a recessed port area insures that x-ray emission from the plasma, as opposed to the wall or limiter, is detected. Emission measurements are shown in Fig. 19-4 for ohmic discharges, and during RF injection at $\bar{n} = 3 \times 10^{12}$ cm^{-3} and $P_{RF} = 20$ kW. The initial ohmic discharge contained a significant runaway tail component and RF injection at this power level did not significantly change the high energy, $\varepsilon_\gamma > 30$ keV, x-ray emission or its spatial profile. The hard x-ray emission is found to be strongly peaked in the center of the plasma with a width of approximately 5 cm, although the actual distribution may be even narrower in view of the spatial resolution of the collimator, 3 cm. It is interesting that the quasilinear theory[2] predicts that instability of a narrow beam should result in a broad spectrum fpi < f < fpe of RF bursts in agreement with experiment.

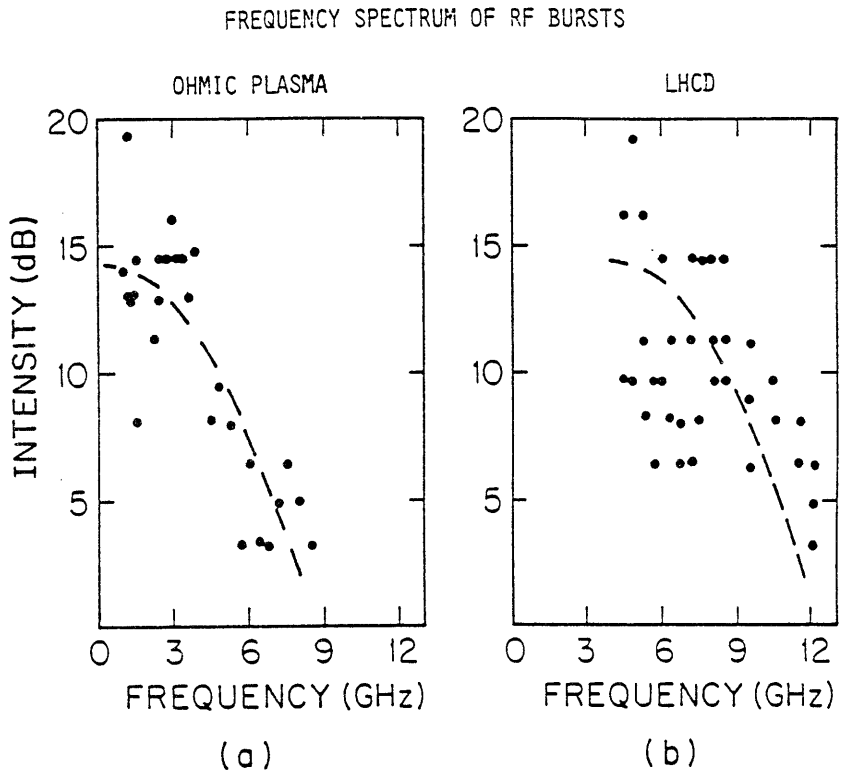

Figure 19-4: Frequncy spectrum of RF bursts with/without LHCD from RF probe in limiter shadow

19.3.6 Ion Heating

Ion heating experiments employing a waveguide grill antenna located at the conventional side position on the midplane of Versator have been completed. At a toroidal field of B_o = 1.4T and density $\bar{n}_e$ = 1.3 - 3 x $10^{13}cm^{-3}$, a poorly confined perpendicular tail in the ion distribution is formed during RF injection. In the density range 2.4 - 2.8 x $10^{13}cm^{-3}$, heating of the ion bulk distribution is occasionally observed; a maximum ion temperature rise of 50 eV for 50 kW transmitted RF power has been recorded. Although ion heating in Versator can be expected to be inefficient on theoretical grounds, the cause of the irreproducibility of the heating results is not well understood.

Recently, initial ion heating investigations have been performed using a grill which launches lower hybrid waves from the top of the Versator plasma. Though this antenna is designed for use in lower-hybrid current-drive experiments, the radial propagation characteristics allowed by this grill are predicted to be beneficial for ion heating as well as current drive, although the launched spectrum of the grill is not optimal for the former. Results to date indicate that, as for the previous grill position, an ion tail with a short confinement time (< 150 μs) is created over roughly the same density range as for the side launching experiments. No bulk heating is measured for transmitted powers of up to 100 kW. Compared to the case with the previous antenna, the ion tails seen in these recent studies are of

lower temperature (0.2 keV versus 1.0 keV) and extend to lower energies (0.4 keV versus 1.2 keV). Contrary to what is qualitatively expected from toroidal ray tracing theory, no significant asymmetry in the fast ion effects with respect to the grill phasing relative to the plasma current is observed.

19.3.7 Diagnostic Experiments

The Versator II tokamak experiments are supported by a complete range of plasma diagnostic experiments. The progress on some of these experiments is summarized as follows:

19.3.8 UV and Visible Diagnostics

Vacuum Ultraviolet (UV) spectroscopy has been used as a routine diagnostic to yield ion temperature during the lower-hybrid ion heating (LHH) experiments. The ion temperature has been obtained by measuring Doppler widths of various impurity line emissions in the UV region (e.g. OVII 1623Å, CV 2271Å, OV 2781Å and CIII 2297Å). Preliminary results from the LHH experiment launching the wave from a top port were not positive. Doppler measurements from UV did not show any significant bulk temperature increase during the RF compared to Ohmic cases; nevertheless, the perpendicular charge-exchange diagnostics showed a tail formation ($\bar{n}_e \sim 2.5 \times 10^{13} cm^{-3}$, $B_T \sim 13$ kg, $I_p \sim$ (50–60) kA, $P_{RF} \sim 100$ kW).

The UV, visible and a H_α photodiode (filter halfwidth 10Å) have been incorporated with lower-hybrid current drive (LHCD) experiments. The UV diagnostics have been used to monitor impurity influxes during the RF. There is no appreciable change of impurity influxes during the RF. The visible monochromator and photo diode detector have been used to measure H_α emissions at various toroidal positions (e.g. the limiter, the gas port, the RF port, etc.). The results show a slight decrease of the 20–40% during the RF; this implies that the volume ionization rate of hydrogen neutrals has also been decreased. Typically, a density increase is observed during LHCD, and since the extra influxes of either neutral hydrogen or impurities decreases or does not change, it is concluded that the particle confinement during current drive probably has increased.

In summary, UV and visible diagnostics have been used in studies of heating efficiency and particle confinement during lower hybrid heating and current drive experiments.

19.3.9 Thomson Scattering

Tokamaks commonly use Thomson scattering to measure profiles of electron temperature, $T_e(r)$, across the minor radius of the plasma. The scattered laser light has a Doppler-broadened spectrum, with a width related to the electron velocity distribution (and hence to T_e) and an intensity proportional to n_e at the laser's focus.

For the past two years, Thomson scattering has been a valuable plasma diagnostic in Versator's various RF (microwave) heating and current drive experiments. The measurements are summarized

below:

In electron cyclotron heating experiments up to 100 kW at 35 GHz, in a mixture of ordinary and extraordinary modes, was injected from the high-field side of the plasma at varying angles to the toroidal field. The consequence was a large ($\leq$ 70%) but irreproducible increase in the bulk electron temperature with the consistent production of a superthermal electron tail. The results were largely independent of wave polarization or the angle of injection.

In lower hybrid ion heating experiments a phased array of waveguides, mounted on the outside wall of the torus, has injected up to 100 kW at 800 MHz. For ion heating, a suitable waveguide spacing and phasing was selected to launch lower hybrid waves with $n_{\parallel} \sim 5.5$ into a high-density ($\bar{n}_e \sim 2.5 \times 10^{13}$ cm^{-3}) plasma. Thomson scattering measurements of electron temperature and density profiles were unchanged by RF in the ion heating density regime. Measurements are planned at lower density during RF current drive.

19.3.10 X-Ray Measurements

In early 1983, a NaI hard x-ray detector, pulse height analysis system was constructed for Versator II. The purpose of this diagnostic is to measure the bremsstrahlung radiation spectrum from the high energy (20 keV - 1 MeV) superthermal electrons present in low density ($\bar{n}_e \leq 1 \times 10^{13}$ cm^{-3}) ohmic and RF current driven discharges.

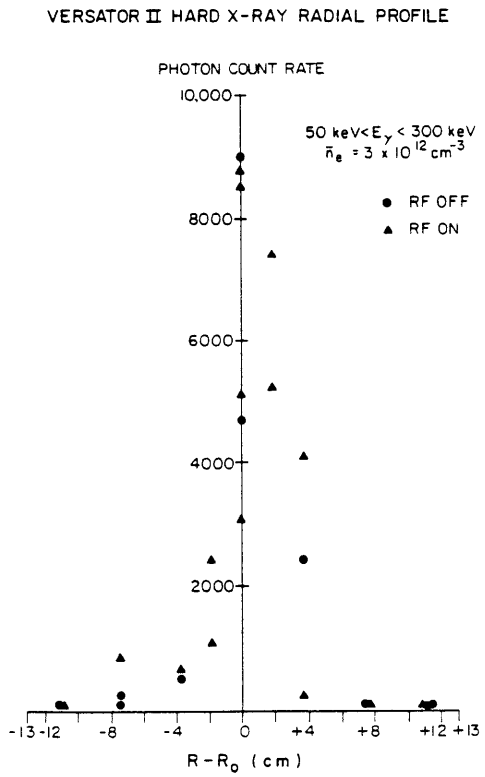

Figure 19-5: Hard x-ray profiles from scanning hard x-ray spectrometer

Typical hard x-ray spectra in the current drive regime ($\bar{n}_e \leq 6 \times 10^{12}$) have slopes of 30–50 keV and maximum detected photon energies of 500–800 keV. The NaI radial profile, scanned from below the torus for E_γ = 50 – 300 keV, is strongly peaked on the major radius (FWHM $\simeq$ 5 cm) for both RF and ohmic plasmas (Fig. 19–5). Time resolved NaI measurements have revealed that this x-ray emission can be dominated by periodic bursts which correlate with the runaway tail anisotropy instability previously observed in Versator LHCD experiments.[3] Using a Si(Li) soft x-ray detector, which scans the plasma cross section from the side, it has been found that the bursting x-ray emission comes primarily from the upper half of the torus. Measurements with the Si(Li) detector PHA system have also been made during lower hybrid electron heating experiments in the density range $\bar{n}_e$ = 1 – 2 x 10^{13}. Although no measurable electron bulk heating has been found with soft x-rays, consistent enhancements of the electron tail (E > 5 keV) are observed (Fig. 19–1). The RF tail intensity profile is peaked on the horizontal midplane (FWHM $\simeq$ 10 cm), but is up/down asymmetric, with the greatest RF enhancement occurring in the upper half of the torus. Presently, x-ray studies are concentrating on the LH current drive density limit by measuring the effect of RF injection on the electron distribution function near the critical density.

References

1. S.C. Luckhardt, M. Porkolab, S. Knowlton, K.-I. Chen, A. Fisher, and F. McDermot, Phys. Rev. Lett. 48, 152 (1982).
2. V.V. Parail and O.P. Pogutse, Nuclear Fusion 18, 3, 303 (1978).
3. S.C. Luckhardt, et al., "Heating of Toroidal Plasmas," 3rd Joint Varenna—Grenoble International Symposium, CEN-Grenoble, France, 2, 529 (1982).
4. P.T. Bonoli and E. Ott, Phys. Fluids 25, 2, 359 (1982).
5. D.W. Ignat, Phys. Fluids 25, 2, 359 (1982).
6. Y. Baranov and V.I. Fedorov, Nuclear Fusion 20, 9, 1111 (1980).
7. N.J. Fisch, Phys. Rev. Lett. 41, 873 (1978).
8. J. Timberlake, et al., J. Vac. Sci. Technology 20, 4, 1309 (1982).

19.4 Physics of Thermonuclear Plasmas

U.S. Department of Energy (Contracts DE-AC02-78ET-51013 and DE-AC02-78ET-53073.A002)
Bruno Coppi

The theme of our research program is the combined experimental and theoretical investigation of plasmas in which fusion reactions have a significant influence on their thermal energy balance and physical properties.

Our characteristic line of interest involves plasmas with relatively high densities, in the range 10^{14} to 10^{15} particles/cm^3, in view of their attractive confinement properties, and magnetic confinement configurations that are suitable to contain the high energy (in the MeV range) charge particles that are produced by fusion reactions. The line of experimental devices that we have developed for this is represented by its prototype, the Alcator A machine, and is characterized by toroidal plasma columns

that can sustain both high currents and current densities. This requirement, leading to adoption of toroidal magnet configurations of compact size and relatively high fields, has made it possible to achieve and maintain the record values for the combined confinement parameters "$nT\tau$", the product of the peak particle pressure nT and the energy replacement time τ, and "$n\tau$". In addition, a sequence of plasma regimes of basic physical interest, in terms of the different characteristics of the particle distributions in velocity space that can be generated and of the collective modes that are excited, has been produced. The conditions where nearly impurity-free plasmas can be obtained have been realized at the same time.

By combining these experimental results with the theoretical analysis of the global transport properties in the plasma regimes that have been attained so far and the known physics of deuterium - tritium fusing plasmas, it has been possible to formulate a research program directed toward studying thermonuclear ignition by a series of compact devices that are called Ignitors.

The conceptual design of one of these devices has been completed in 1982 and has been successfully reviewed by an international panel convened by the C.E.C. (Euratom). This was chaired by Sr. John Adams (CERN), and the other members were R. Bickerton (JET), P. Reardon (Princeton), P. Rebut (JET), and M.N. Rosenbluth (U. Texas).

An independent program involving a compact device that has about the same philosophy and dimensions as Ignitor but gives a more enhanced role to heating by adiabatic compression is already underway in the Soviet Union. In fact the subject of compact ignition experiments has been the theme of an official U.S.-U.S.S.R. exchange held in July 1982 at Moscow and Leningrad with the participation of two of us (B. Coppi and R. Parker).

In 1980 we pointed out the feasibility of experimental fusion reactors that do not utilize tritium as a primary fuel, but are based on reactions such as D-He^3 that do not produce neutrons. These ideas have generated widespread interest and this has been enhanced in 1982 by the beginning of a serious[2,3] effort to investigate whether plasmas with spin polarized nuclei can be used as fuels in order to decrease further the already low fraction of energy produced in the form of neutrons in D-He^3 reactors. In fact the results of our studies indicate that an experimental program for an analysis of the "burn" conditions for these so-called advanced fuels can be undertaken with present day technologies and on the basis of existing knowledge of the physics of magnetically confined plasmas.[1]

One of the necessary conditions for (the feasibility of) these experiments is to produce plasmas in which the peak plasma pressure is a finite fraction of the magnetic pressure without exciting macroscopic instabilities. In early 1978 we took a first step in this direction when we demonstrated the existence of a "second stability" region that is relevant to these experiments, regarding the onset of a set of modes, so-called "ballooning".[4,5] These had been thought previously to severely limit the value of the plasma pressure relative to that of the confining magnetic field. Following a similar line of

thinking, in 1981 we reported that another important class of modes, the so-called "internal kinks" also tend to become stable[6] in a second-stability region. This region of stability overlaps the corresponding one of "ballooning" modes. Therefore, now we can invision a sequence of plasma equilibria[7] that involve increasing values of the plasma temperature and remain macroscopically stable while the desired thermonuclear burn conditions are achieved.

At relatively low plasma densities, lower than 10^{13} particles/cm, where the plasma current induced by the applied d.c. electric field is carried by superthermal electrons, a regime labelled the "slide-away", was first identified[8] by a series of experiments carried out in 1974 and 1975 on the Alcator A machine. Recently, a similar regime has been observed to be induced by the appropriate injection of microwaves at the so-called lower hybrid frequency. A series of successful experiments that have produced this form of "current drive" have been carried out both on the Versator II and the Alcator C devices. In fact, current drive has been observed for record high densities with the latter experimental device while appropriate analytical and numerical models for the physical processes involved have been formulated.

As is traditional with our mode of operation, during 1982 we have maintained an effective system of close collaborations with national and overseas institutions for both our theoretical and experimental program. Our contributions have been presented at major national and international meetings.

References

1. B. Coppi, M.I.T./R.L.E. Report PRR-80/24 (1980).
2. R.M. Kulsrud, H.P. Furth, E.J. Valeo, and M. Goldhaber, "Fusion Reactor Plasmas with Polarized Nuclei," Phys. Rev. Lett. 49, 1248 (1982).
3. B. Coppi, F. Pegoraro, and J. Ramos, "Instability of Fusing Plasmas and Relevant Depolarization Process," paper submitted for the 1983 Sherwood Theory Meeting, Washington, D.C., March 1983.
4. B. Coppi and M.N. Rosenbluth, in Plasma Physics and Controlled Nuclear Fusion Research (1965), Vol. 1 (International Atomic Energy Agency, Vienna, 1966) p. 617.
5. B. Coppi, G.B. Crew, and J.J. Ramos, Comments Pl. Phys. Contr. Fus. Res. 6, 109 (1981).
6. G.B. Crew and J.J. Ramos, Phys. Rev. A 426, 1149 (1982).
7. B. Coppi, G. Crew, and J. Ramos, M.I.T./R.L.E. Report PTP-82/6 (1982) to be published in Comments Pl. Phys. Cont. Fus. Res.
8. B. Coppi, A. Oomens, R. Parker, L. Pieroni, F. Schuller, S. Segre, and R. Taylor, M.I.T./R.L.E. Report PRR-74/18 (1974).